Production of the neutral top-pion π_t^0 in association with a high-p_T jet at the LHC*

ZHU Shi-Hai(朱世海) YUE Chong-Xing(岳崇兴)[1)] LIU Wei(刘伟) DING Li(丁丽)

(Department of Physics, Liaoning Normal University, Dalian 116029, China)

Abstract In the framework of the topcolor-assisted technicolor (TC2) model, we study the production of the neutral top-pion π_t^0 in association with a high-p_T jet at the LHC, which proceeds via the partonic processes $gg \longrightarrow \pi_t^0 g$, $gq \longrightarrow \pi_t^0 q$, $q\bar{q} \longrightarrow \pi_t^0 g$, $gb(\bar{b}) \longrightarrow \pi_t^0 b(\bar{b})$, and $b\bar{b} \longrightarrow \pi_t^0 g$. We find that it is very challenging to detect the neutral top-pion π_t^0 via the process $pp \longrightarrow \pi_t^0 + jet + X \rightarrow t\bar{t} + jet + X$, while the possible signatures of π_t^0 might be detected via the process $pp \longrightarrow \pi_t^0 + jet + X \rightarrow (\bar{t}c + t\bar{c}) + jet + X$ at the LHC.

Key words neutral top-pion, LHC, production cross section

PACS 12.60.Cn, 14.80.Cp, 12.15.Lk

1 Introduction

The Higgs mechanism for the electroweak symmetry breaking (EWSB) is still an untested part of the Standard Model (SM). Searching for the SM Higgs boson is one of the main tasks of the forthcoming Large Hadron Collider (LHC), which has a considerable capability to discover and measure almost all of its quantum properties[1]. However, if the LHC finds evidence for a new scalar state, it may not necessarily be the SM Higgs boson. Most of the new physics models beyond the SM predict the existence of new scalar states. These new particles may have production cross sections and branching ratios which differ from those of the SM Higgs boson. Distinguishing the various new physics scenarios is an important task for the current and near future high energy collider experiments. Thus, studying the production and decay of the new scalar states at the LHC is of special interest.

Due to the large gluon luminosity, the main production mechanism for a scalar Higgs boson at the LHC is the partonic gluon fusion process $gg \rightarrow H$[2], which is the so-called inclusive single Higgs boson production channel. In order to fully explore the Higgs detection capabilities of the LHC, one should investigate more exclusive channels, like e.g. Higgs production in association with a high-p_T hadronic jet[3]. The main advantage of this channel is the richer kinematical structure of the events which allows for refined cuts increasing the signal-to-background ratio. So far, this production channel has been extensively studied in the SM[4, 5]. In the minimal supersymmetric standard model (MSSM), the analogous process, i.e. scalar Higgs production in association with a high-p_T jet was also extensively studied in Refs. [6, 7].

Among various kinds of dynamical EWSB theories, the topcolor scenario is attractive because it can explain the large top quark mass and provides a possible EWSB mechanism[8]. The topcolor-assisted technicolor (TC2) model[9] is one of the phenomenologically viable models, which has all the essential features of the topcolor scenario. This model predicts three CP odd top-pions (π_t^0, $\pi_t^{\pm}$) with large Yukawa couplings to the third family. The aim of this paper is to consider the production of the neutral top-pion π_t^0 associated with a high-p_T jet and compare our results with those for the Higgs boson from the SM or the MSSM. We hope that our work can help the upcoming LHC to test the topcolor scenario and to differentiate various kinds of new physics models.

In the rest of this paper, we will give our results in detail. In Section 2, we will calculate the production cross section of the hadronic process $pp \longrightarrow \pi_t^0$+jet+X and give a simply phenomenological analysis at the LHC. Our conclusion is represented in Section 3.

Received 28 December 2008, Revised 6 January 2009

* Supported by NSFC (10675057), and Foundation of Liaoning Educational Committee (2007T086)

1) E-mail: cxyue@lnnu.edu.cn

2 Production of the neutral top-pion π_t^0 associated with a high-p_T jet

In the TC2 model[9], the topcolor interactions, which are not flavor-universal and mainly couple to the third generation fermions, generally generate small contributions to EWSB and give rise to the main part of the top quark mass. Thus, the top-pions $\pi_t^{0,\pm}$ have large Yukawa couplings to the third generation fermions. Such features can result in large tree-level flavor changing couplings of the top-pions to the fermions when one writes the interactions in the fermion mass eigen-basis. Just as for the SM Higgs boson, the couplings of the top-pion to a pair of quarks are in proportion to the quark masses. The explicit form for the couplings of the neutral top-pion π_t^0 to quarks, which are related to our calculation, can be written as[9, 10]:

$$\frac{\mathrm{i}m_t}{\sqrt{2}F_t}\frac{\sqrt{\nu_W^2-F_t^2}}{\nu_W}[k_{UR}^{tt}k_{UL}^{tt*}\bar{t}\gamma^5 t\pi_t^0+ \frac{m_b-m_b'}{m_t}\bar{b}\gamma^5 b\pi_t^0+k_{UR}^{tc*}k_{UL}^{tt}\bar{t}P_R c\pi_t^0], \quad (1)$$

where $\nu_W=\nu/\sqrt{2}\approx 174$ GeV, $P_R=(1+\gamma^5)/2$ is the right-handed projection operator, $F_t\approx 50$ GeV is the top-pion decay constant, and $m_b'\approx 0.1\varepsilon m_t$ is the part of the bottom quark mass generated by extended technicolor interactions. $k_{UL(R)}$ are the rotation matrices that diagonalize the up-quark mass matrix M_U for which the Cabibbo-Kobayashi-Maskawa (CKM) matrix is defined as $V_{CKM}=k_{UL}^{+}k_{DL}$. To yield a realistic form of V_{CKM}, it has been shown that the values of the matrix elements $k_{UL(R)}^{ij}$ can be taken as[10]:

$$k_{UL}^{tt}\approx 1,\quad k_{UR}^{tt}=1-\varepsilon,\quad k_{UR}^{tc}\leqslant\sqrt{2\varepsilon-\varepsilon^2}\,. \quad (2)$$

In our numerical estimation, we will take $k_{UR}^{tc}=\sqrt{2\varepsilon-\varepsilon^2}$ and take ε as a free parameter, which is assumed to be in the range of 0.01—0.1.

Similar to the Higgs boson predicted by the SM or the MSSM, the neutral top-pion π_t^0 can be produced at the LHC in association with a high-p_T jet through three partonic processes: gluon fusion ($gg\longrightarrow g\pi_t^0$), quark-gluon scattering ($q(\bar{q})g\longrightarrow q(\bar{q})\pi_t^0$), and quark-antiquark annihilation ($q\bar{q}\longrightarrow g\pi_t^0$). Although the gluon fusion and quark-gluon scattering partonic processes give main contributions to the production cross section for the hadronic process $pp\longrightarrow\pi_t^0+\mathrm{jet}+X$ at the LHC, our numerical analysis includes all of the above three processes, which proceed at one-loop, as shown in Fig. 1(a)—(e). Considering the small value of the decay constant F_t and the relatively large bottom-quark mass, we also consider the contributions of the tree-level partonic processes $gb\longrightarrow\pi_t^0 b$ and $b\bar{b}\longrightarrow\pi_t^0 g$, as shown in Fig. 1(f)—(h).

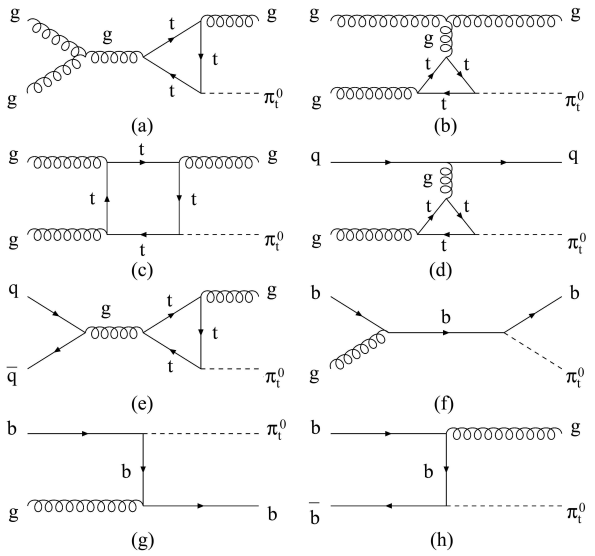

Fig. 1. Feynman diagrams for the partonic processes contributing to the hadronic process $pp\rightarrow\pi_t^0+\mathrm{jet}+X$ at the leading order. The other diagrams obtained by exchanging the gluons or exchanging π_t^0 are not shown here.

The variant amplitudes corresponding to the Feynman diagrams as shown in Fig. 1 can be written as:

$$M_{(a)}=\frac{\mathrm{i}}{4\sqrt{2}\pi^2}T_{ij}^{c_3}T_{ji}^{c_4}f^{c_1c_2c_3}g_s^3\frac{m_t^2(1-\varepsilon)\sqrt{\nu_W^2-F_t^2}}{F_t\nu_W(p_1+p_2)^2}C_{0(a)}[(p_2-p_1)_\mu\epsilon(p_1)\cdot\epsilon(p_2)+ (-2p_2-p_1)\cdot\epsilon(p_1)\epsilon_\mu(p_2)+(2p_1+p_2)\cdot\epsilon(p_2)\epsilon_\mu(p_1)]\epsilon^{\mu\nu\rho\sigma}p_{3\rho}p_{4\sigma}\epsilon_\nu(p_3), \quad (3)$$

$$M_{(b)}=\frac{\mathrm{i}}{4\sqrt{2}\pi^2}T_{ij}^{c_3}T_{ji}^{c_4}f^{c_1c_2c_3}g_s^3\frac{m_t^2(1-\varepsilon)\sqrt{\nu_W^2-F_t^2}}{F_t\nu_W(p_1-p_3)^2}C_{0(b)}[(-p_2-p_1)\cdot\epsilon(p_3)\epsilon_\mu(p_1)+ (p_2-p_3)\cdot\epsilon(p_1)\epsilon_\mu(p_3)+(p_3+p_1)_\mu\epsilon(p_1)\cdot\epsilon(p_3)]\epsilon^{\mu\nu\rho\sigma}p_{4\rho}(p_1-p_3)_\sigma\epsilon_\nu(p_2), \quad (4)$$

$$
\begin{aligned}
M_{(\rm c)} =\ & \frac{\rm i}{4\sqrt{2}\pi^2}T^{\rm c_1}_{\rm ij}T^{\rm c_2}_{\rm jk}T^{\rm c_3}_{\rm ki}g_{\rm s}^3\frac{m_{\rm t}(1-\varepsilon)\sqrt{\nu_{\rm W}^2-F_{\rm t}^2}}{F_{\rm t}\nu_{\rm W}}\times \\
& (-D_{0(\rm c)}m_{\rm t}^3\epsilon^{\mu\nu\rho\sigma}p_{1\sigma}+D_{0(\rm c)}m_{\rm t}^3\epsilon^{\mu\nu\rho\sigma}p_{4\sigma}-D_{0(\rm c)}m_{\rm t}\epsilon^{\rho\sigma\alpha\beta}p_{1\sigma}p_{2\alpha}p_{4\beta}g^{\mu\nu}+ \\
& D_{0(\rm c)}m_{\rm t}\epsilon^{\nu\sigma\alpha\beta}p_{1\sigma}p_{2\alpha}p_{4\beta}g^{\mu\rho}-D_{0(\rm c)}m_{\rm t}\epsilon^{\nu\rho\sigma\alpha}p_1^{\mu}p_{2\sigma}p_{4\alpha}+D_{0(\rm c)}m_{\rm t}\epsilon^{\nu\rho\sigma\alpha}p_{1\sigma}p_{4\alpha}p_2^{\mu}- \\
& D_{0(\rm c)}m_{\rm t}\epsilon^{\nu\rho\sigma\alpha}p_{1\sigma}p_{2\alpha}p_4^{\mu}-D_{0(\rm c)}m_{\rm t}\epsilon^{\mu\sigma\alpha\beta}p_{1\sigma}p_{2\alpha}p_{4\beta}g^{\nu\rho}+2D^{\nu}_{(\rm c)}m_{\rm t}\epsilon^{\mu\rho\sigma\alpha}p_{1\sigma}p_{4\alpha}+ \\
& 2D^{\nu}_{(\rm c)}m_{\rm t}\epsilon^{\mu\rho\sigma\alpha}p_{2\sigma}p_{4\alpha}+D_{0(\rm c)}m_{\rm t}\epsilon^{\mu\rho\sigma\alpha}p_{2\sigma}p_{4\alpha}p_1^{\nu}-D_{0(\rm c)}m_{\rm t}\epsilon^{\mu\rho\sigma\alpha}p_{1\sigma}p_{4\alpha}p_2^{\nu}+ \\
& D_{0(\rm c)}m_{\rm t}\epsilon^{\mu\rho\sigma\alpha}p_{1\sigma}p_{2\alpha}p_4^{\nu}-2D^{\nu}_{(\rm c)}m_{\rm t}\epsilon^{\mu\rho\sigma\alpha}p_{2\sigma}p_{4\alpha}-D_{0(\rm c)}m_{\rm t}\epsilon^{\mu\nu\sigma\alpha}p_{2\sigma}p_{4\alpha}p_1^{\rho}- \\
& D_{0(\rm c)}m_{\rm t}\epsilon^{\mu\nu\sigma\alpha}p_{1\sigma}p_{4\alpha}p_2^{\rho}+D_{0(\rm c)}m_{\rm t}\epsilon^{\mu\nu\sigma\alpha}p_{1\sigma}p_{2\alpha}p_4^{\rho}+D_{\nu(\rm c)}D^{\nu}_{(\rm c)}m_{\rm t}\epsilon^{\mu\nu\rho\sigma}p_{1\sigma}- \\
& D_{\nu(\rm c)}D^{\nu}_{(\rm c)}m_{\rm t}\epsilon^{\mu\nu\rho\sigma}p_{4\sigma}-2D_{\nu(\rm c)}\cdot p_2m_{\rm t}\epsilon^{\mu\nu\rho\sigma}p_{1\sigma}+2D_{\nu(\rm c)}\cdot p_2m_{\rm t}\epsilon^{\mu\nu\rho\sigma}p_{4\sigma}- \\
& 2D_{\nu(\rm c)}\cdot p_4m_{\rm t}\epsilon^{\mu\nu\rho\sigma}p_{2\sigma}+D_{0(\rm c)}p_1\cdot p_2m_{\rm t}\epsilon^{\mu\nu\rho\sigma}p_{4\sigma}-D_{0(\rm c)}p_1\cdot p_4m_{\rm t}\epsilon^{\mu\nu\rho\sigma}p_{2\sigma}+ \\
& D_{0(\rm c)}p_2\cdot p_2m_{\rm t}\epsilon^{\mu\nu\rho\sigma}p_{1\sigma}-D_{0(\rm c)}p_2\cdot p_4m_{\rm t}\epsilon^{\mu\nu\rho\sigma}p_{1\sigma})\epsilon_{\mu}(p_1)\epsilon_{\nu}(p_2)\epsilon_{\rho}(p_3), \qquad (5)
\end{aligned}
$$

$$
M_{(\rm d)} = \frac{1}{4\sqrt{2}\pi^2}T^{\rm c_1}_{\rm ij}T^{\rm c_1}_{\rm kl}T^{\rm c_2}_{\rm lk}g_{\rm s}^3\frac{m_{\rm t}^2(1-\varepsilon)\sqrt{\nu_{\rm W}^2-F_{\rm t}^2}}{F_{\rm t}\nu_{\rm W}(p_1-p_3)^2}C_{0(\rm d)}\bar{u}(p_3)\gamma^{\mu}u(p_1)g_{\mu\nu}\epsilon^{\nu\lambda\rho\sigma}p_{4\rho}(p_1-p_3)_{\sigma}\epsilon_{\lambda}(p_2), \qquad (6)
$$

$$
M_{(\rm e)} = \frac{1}{4\sqrt{2}\pi^2}T^{\rm c_1}_{\rm ij}T^{\rm c_1}_{\rm kl}T^{\rm c_2}_{\rm lk}g_{\rm s}^3\frac{m_{\rm t}^2(1-\varepsilon)\sqrt{\nu_{\rm W}^2-F_{\rm t}^2}}{F_{\rm t}\nu_{\rm W}(p_1+p_2)^2}C_{0(\rm e)}\bar{u}(p_2)\gamma^{\mu}v(p_1)g_{\mu\nu}\epsilon^{\nu\lambda\rho\sigma}p_{3\rho}p_{4\sigma}\epsilon_{\lambda}(p_3), \qquad (7)
$$

$$
M_{(\rm f)} = \frac{1}{\sqrt{2}}T^{\rm c_1}_{\rm ij}g_{\rm s}\frac{1}{(p_1+p_2)^2-m_{\rm b}^2}\frac{m_{\rm b}-m'_{\rm b}}{F_{\rm t}}\frac{\sqrt{\nu_{\rm W}^2-F_{\rm t}^2}}{\nu_{\rm W}}\bar{u}(p_3)\gamma^5(\not{p}_1+\not{p}_2-m_{\rm b})\gamma^{\mu}u(p_1)\epsilon_{\mu}(p_2), \qquad (8)
$$

$$
M_{(\rm g)} = \frac{1}{\sqrt{2}}T^{\rm c_1}_{\rm ij}g_{\rm s}\frac{1}{(p_1-p_3)^2-m_{\rm b}^2}\frac{m_{\rm b}-m'_{\rm b}}{F_{\rm t}}\frac{\sqrt{\nu_{\rm W}^2-F_{\rm t}^2}}{\nu_{\rm W}}\bar{u}(p_4)\gamma^{\mu}(\not{p}_1-\not{p}_3-m_{\rm b})\gamma^5u(p_1)\epsilon_{\mu}(p_2), \qquad (9)
$$

$$
M_{(\rm h)} = \frac{1}{\sqrt{2}}T^{\rm c_1}_{\rm ij}g_{\rm s}\frac{1}{(p_1-p_3)^2-m_{\rm b}^2}\frac{m_{\rm b}-m'_{\rm b}}{F_{\rm t}}\frac{\sqrt{\nu_{\rm W}^2-F_{\rm t}^2}}{\nu_{\rm W}}\bar{v}(p_2)\gamma^{\mu}(\not{p}_1-\not{p}_3-m_{\rm b})\gamma^5u(p_1)\epsilon_{\mu}(p_4). \qquad (10)
$$

Here p_1, p_2 are the momenta of the incoming states, and p_3, p_4 are the momenta of the outgoing final states. The $T^{\rm c}_{\rm ij}$ are the $SU(3)$ color matrices and the $f^{\rm c_1c_2c_3}$ are the antisymmetric $SU(3)$ structure constants in which i, j are the color indices and $\rm c_1$, $\rm c_2$, $\rm c_3$ are the indices of gluon. The three-point and four-point standard functions C_0, D_0, D_1, D_ν [11, 12] for different Feynman diagrams are defined as:

$$
\begin{aligned}
C_{0(\rm a)} &= C_{0(\rm a)}(p_1+p_2,-p_3,m_{\rm t},m_{\rm t},m_{\rm t}),\\
C_{0(\rm b)} &= C_{0(\rm b)}(p_1-p_3,p_2,m_{\rm t},m_{\rm t},m_{\rm t}),\\
C_{0(\rm d)} &= C_{0(\rm d)}(p_1-p_3,p_2,m_{\rm t},m_{\rm t},m_{\rm t}),\\
C_{0(\rm e)} &= C_{0(\rm e)}(p_1+p_2,-p_3,m_{\rm t},m_{\rm t},m_{\rm t});\\
D_{0(\rm c)} &= D_{0(\rm c)}(p_1,p_2,-p_3,m_{\rm t},m_{\rm t},m_{\rm t},m_{\rm t}),\\
D_{1(\rm c)} &= D_{1(\rm c)}(p_1,p_2,-p_3,m_{\rm t},m_{\rm t},m_{\rm t},m_{\rm t}),\\
D_{\nu(\rm c)} &= p_{1\nu}*D_{1(\rm c)}(1)+p_{2\nu}*D_{1(\rm c)}(2)+p_{3\nu}*D_{1(\rm c)}(3).
\end{aligned}
$$

Each loop diagram is composed of some scalar loop functions, which are calculated by using LoopTools[12].

The hadronic cross section at the LHC is obtained by convoluting the partonic cross sections with the parton distribution functions (PDFs). In our numerical calculation, we will use CTEQ6L PDFs[13] for the gluon and quark PDFs. The renormalization scale $\mu_{\rm R}$ and the factorization scale $\mu_{\rm F}$ are chosen to be $\mu_{\rm R}=\mu_{\rm F}=m_{\pi_{\rm t}}$ for the gluons and the light quarks, and to be $\mu_{\rm R}=\mu_{\rm F}=m_{\pi_{\rm t}}/4$ for the bottom-quark, in which $m_{\pi_{\rm t}}$ is the mass of the neutral top-pion $\pi_{\rm t}^0$. To make our predictions more realistic and the high-$p_{\rm T}$ jet not too close to the beam axis, we require that the transverse momentum $p_{\rm T}$ and pseudorapidity η of the hadronic jet satisfy: $p_{\rm T}>30$ GeV and $|\eta|<4.5$, which have been used in previous MSSM studies for the LHC[6, 7].

From the above discussions we can see that the production cross section σ for the hadronic process $\rm pp\to\pi_{\rm t}^0+jet+X$ is dependent on the free parameters ε and $m_{\pi_{\rm t}}$. Similar to Ref. [14], we will assume that the free parameters ε and $m_{\pi_{\rm t}}$ are in the range of 0.01—0.1 and 200—500 GeV, respectively.

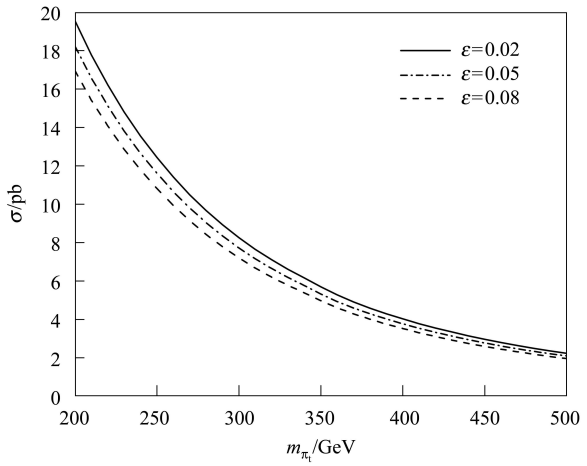

Fig. 2. The total cross section of the hadronic process $pp \to \pi_t^0 + jet + X$ as a function of the π_t^0 mass m_{π_t} for three values of the free parameter ε.

Our numerical results are shown in Fig. 2, in which we plot the cross section σ as a function of the mass parameter m_{π_t} for three values of the parameter ε. One can see from Fig. 2 that σ is insensitive to the free parameter ε. For $\varepsilon = 0.05$ and 200 GeV$\leqslant m_{\pi_t} \leqslant$500 GeV, the value of the production cross section σ is in the range of 18.3—2.1 pb. Observably, if we assume that the π_t^0 mass m_{π_t} is equal to that of the SM Higgs boson H or the MSSM Higgs boson H^0, the cross section for the production of the neutral top-pion π_t^0 associated with a high-p_T is significantly larger than that of the SM Higgs boson H[4, 5] or the MSSM Higgs boson H^0[6, 7]. This is because the $\pi_t^0 t\bar{t}$ coupling is larger than that for the SM Higgs boson H or the MSSM Higgs boson H^0.

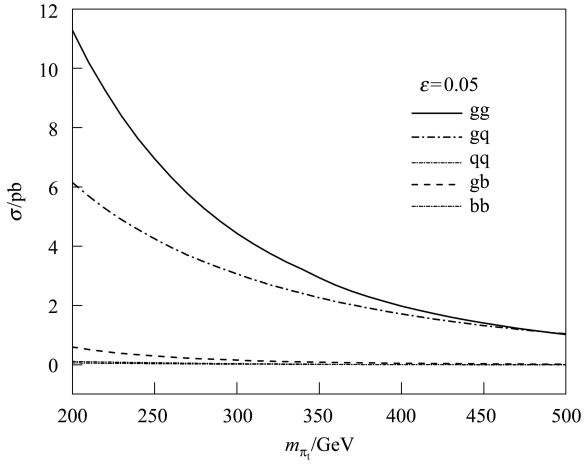

Fig. 3. The hadronic cross sections for different partonic processes as a function of the π_t^0 mass m_{π_t} for the free parameter $\varepsilon = 0.5$.

To see contributions of the different partonic processes to the total hadronic cross section, we plot the hadronic cross sections of the partonic processes $gg \to \pi_t^0 g$, $qg \to q\pi_t^0$ ($q = u, c, d, s, \bar{u}, \bar{c}, \bar{d}, \bar{s}$), $q\bar{q} \to \pi_t^0 g$ ($q = u, c, d, s$), $gb(\bar{b}) \longrightarrow \pi_t^0 b(\bar{b})$, and $b\bar{b} \longrightarrow \pi_t^0 g$ for ε=0.05 in Fig. 3. We see that the production of the neutral top-pion π_t^0 in association with a high-p_T jet is dominated by the partonic process $gg \to \pi_t^0 g$, which is similar to the Higgs boson production associated with a high-p_T in the SM and the MSSM. However, for the MSSM model, the contributions of the $b\bar{b}$ channel can be significantly larges, depending on the free parameters. However, this is not the case for the TC2 model. For $0.02 \leqslant \varepsilon \leqslant 0.08$ and 200 GeV $\leqslant m_{\pi_t} \leqslant$ 500 GeV, the hadronic cross section for the partonic process $b\bar{b} \longrightarrow \pi_t^0 g$ is only in the range of 1.6—46 fb, which is several orders of magnitude smaller than that for the partonic process $gg \to \pi_t^0 g$.

It is well known that the mass of the SM Higgs boson H is generally smaller than 200 GeV, one can use the decay channels $H \to \gamma\gamma$, $H \to \tau^+\tau^-$ or $H \to W^+W^-$ to consider the SM Higgs boson signatures generated by the hadronic process $pp \longrightarrow H + jet + X$ at the LHC[5]. For the neutral top-pion π_t^0, its main decay modes are $t\bar{t}$, $\bar{t}c(t\bar{c})$, $b\bar{b}$, gg, and $\gamma\gamma$. For $m_t \leqslant m_{\pi_t} \leqslant 2m_t$, π_t^0 mainly decays to $\bar{t}c$ and $t\bar{c}$. It has been shown that the value of the branching ratio $Br(\pi_t^0 \to \bar{t}c + t\bar{c})$ is larger than 90% for $m_{\pi_t} = 250$ GeV and $\varepsilon \geqslant 0.02$[15]. Thus, for $m_t < m_{\pi_t} \leqslant 2m_t$, the production of neutral top-pion π_t^0 associated with a high-p_T hadronic jet can easily transfer to the tc+jet event. This final state generates characteristic signatures at the LHC experiments. So we further calculate its production rate. We find that, for $\varepsilon \leqslant 0.08$ and $m_{\pi_t} \leqslant 350$ GeV, the production cross section of the hadronic process $pp \to (\bar{t}c + t\bar{c}) + jet + X$ is larger

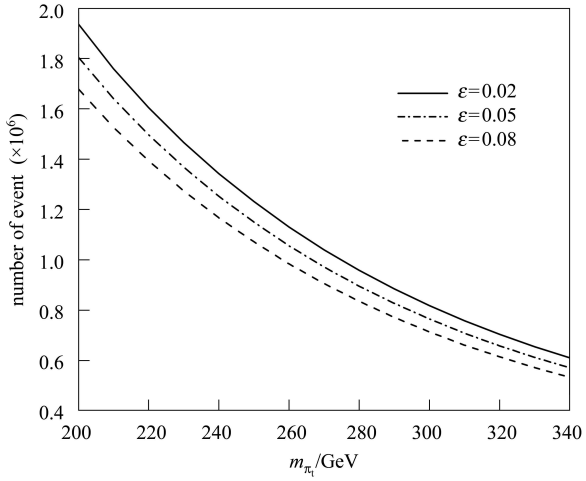

Fig. 4. The number of the tc+jet event as a function of the π_t^0 mass m_{π_t} for three values of the parameter ε.

than 19.4 pb. If we assume the yearly integrated luminosity $\mathcal{L}_{int} = 100\,fb^{-1}$ for the LHC with $\sqrt{s} = 14$ TeV, then there will be $1.94\times10^6 \sim 5.3\times10^5$ tc+jet events to be generated per year for $0.02 \leqslant \varepsilon \leqslant 0.08$ and $200\ \text{GeV} \leqslant m_{\pi_t} \leqslant 340\ \text{GeV}$, as shown in Fig. 4.

For the tc+jet event, the peak of the invariant mass distribution of tc is narrow. To identify tc, one needs to reconstruct the top quark from its main decay mode Wb and the b-tagging and c-tagging are also needed. Furthermore, in the case of the W hadronic decay, the tc+jet event will generate the bjjcj final state, while for the W leptonic decay, it will generate the blνcj final state. For the former final state, the SM background is jjjjj and the SM backgrounds of the later final state mainly come from the $t\bar{t}$, tW and Wjjj production process, which have been analyzed in Ref. [16]. They have shown that suitable kinematical cuts on the observed particles are more than enough to obtain a clear and statistically meaningful flavor-changing signal. Thus we expect that the possible signatures of the neutral top-pion π_t^0 might be detected via the decay channel $\pi_t^0 \to \bar{t}c + t\bar{c}$ at the LHC experiments.

For $m_{\pi_t} > 2m_t$, the neutral top-pion π_t^0 mainly decays to $t\bar{t}$ and the hadronic process $pp \to \pi_t^0 + jet + X$ can give rise to the $t\bar{t}$+jet event. Its production rate can reach 15 pb for $m_{\pi_t} \geqslant 400$ GeV and $\varepsilon \leqslant 0.08$. This kind of event has been calculated at NLO in the SM[17]. It has shown that, for the renormalization and factorization scales having $\mu_R = \mu_F = \mu = m_t$, the NLO cross section for $t\bar{t}$+jet production at the LHC is larger than 500 pb. Thus, the production cross section of the $t\bar{t}$+jet final state coming from TC2 is smaller than that coming from the SM by at least two orders of magnitude. It is very challenging to detect the possible signals of π_t^0 via the process $pp \longrightarrow \pi_t^0 + jet + X \to t\bar{t} + jet + X$.

3 Conclusion

The production of a scalar state (the SM Higgs boson, the MSSM Higgs boson, etc) associated with a high-p_T jet allows for refined cuts increasing the signal-to-background ratio, which is considered advantageous for scalar detection even though its production rate is lower than that for totally inclusive single scalar state production. In the context of the TC2 model, we consider the production of the neutral top-pion π_t^0 accompanied by a high-p_T jet at the LHC. This production channel proceeds by the partonic processes $gg \longrightarrow \pi_t^0 g$, $gq \longrightarrow \pi_t^0 q$, $q\bar{q} \longrightarrow \pi_t^0 g$, $gb(\bar{b}) \longrightarrow \pi_t^0 b(\bar{b})$, and $b\bar{b} \longrightarrow \pi_t^0 g$. We find that, for m_{π_t} equaling the mass of the scalar sate predicted by the MSSM, the hadronic production cross section of the process $pp \longrightarrow \pi_t^0 + jet + X$ is much larger than that for the MSSM scalar state. For $m_t < m_{\pi_t} \leqslant 2m_t$, the main decay channel is $\pi_t^0 \to \bar{t}c + t\bar{c}$. There will be a large number of the tc+jet events to be generated which can generate characteristic signal at the LHC experiment. So we might detect the possible signatures of the neutral top-pion π_t^0 via the process $pp \longrightarrow \pi_t^0 + jet + X \to (\bar{t}c + t\bar{c}) + jet + X$ at the LHC.

Shi-Hai Zhu would like to thank Lei Wang for useful discussions.

References

1 Adam N E et al. arXiv: 0803.1154[hep-ph]
2 Georgi H M, Glashow S L, Machacek M E, Nanopoulos D V. Phys. Rev. Lett., 1978, **40**: 692
3 Chaichian M, Liede I, Lindfors J, Roy D P. Phys. Lett. B, 1987, **198**: 416; 1988, **205**: 595; Ellis R K, Hinchliffe I, Soldate M, van der Bij J J. Nucl. Phys. B, 1988, **297**: 221; Baur U, Nigel Glover E W. Nucl. Phys. B, 1990, **339**: 38
4 Abdellin S et al. Phys. Lett. B, 1998, **431**: 410; Mellado B, Quayle W, WU S L. Phys. Lett. B, 2005, **611**: 60; Phys. Rev. D, 2007, **76**: 093007
5 Anastasiou C, Melnikov K, Petriello F. Phys. Rev. Lett., 2004, **93**: 262002; Nucl. Phys. B, 2005, **724**: 197; Bozzi G, Catani S, de Florian D, Grazzini M. Phys. Lett. B, 2003, **564**: 65; Catani S, de Florian D, Grazzini M, Nason P. JHEP, 2003, **0307**: 028; de Florian D, Grazzini M, Kunszt Z. Phys. Rev. Lett., 1999, **82**: 5209; de Florian D, Kunszt Z, Vogelsang W. JHEP, 2006, **0602**: 047
6 Brein O, Hollik W. Phys. Rev. D, 2003, **68**: 095006; Field B, Dawson S, Smith J. Phys. Rev. D, 2004, **69**: 074013; Langenegger U, Spira M, Statradumov A, Trucb P. JHEP, 2006, **0606**: 035
7 Brein O, Hollik W. Phys. Rev. D, 2007, **76**: 035002; Bonciani K, Degrassi G, Vicini A. JHEP, 2007, **0711**: 095; Brein O, Hollik W. arXiv: 0710.4781[hep-ph]
8 Hill C T, Simmons E H. Phys. Rept., 2003, **381**: 235; 2004, **390**: 553
9 Hill C T. Phys. Lett. B, 1995, **345**: 483; Lane K D, Eichten E. Phys. Lett. B, 1995, **352**: 382; Lane K D. Phys. Lett. B, 1998, **433**: 96; Cvetic G. Rev. Mod. Phys., 1999, **71**: 513
10 Burdman G. Phys. Rev. Lett., 1999, **83**: 2888; HE H J, YUAN C P. Phys. Rev. Lett., 1999, **83**: 28; HE H J, Kanemura S, YUAN C P. Phys. Rev. Lett., 2002, **89**: 101803
11 't Hooft G, Veltman M J G. Nucl. Phys. B, 1979, **153**: 365
12 Hahn T, Perez-Victora M. Comput. Phys. Commun., 1999, **118**: 153; Hahn T. Nucl. Phys. Proc. Suppl., 2004, **135**: 333
13 Pumplin J et al (CTEQ Collaboration). JHEP, 2006, **2**: 032
14 YUE C X, ZONG Z J, XU L L, CHEN J X. Phys. Rev. D, 2006, **73**: 015006
15 YUE C X, KUANG Y P, LU G G. J. Phys. G, 1997, **23**: 163; YUE C X, XU Q J, LIU G L, LI J T. Phys. Rev. D, 2001, **63**: 115002
16 del Aguila F, Aguilar-Saavedra J A. Nucl. Phys. B, 2000, **576**: 56
17 Diffmaier S, Uwer P, Weinzierl S. Phys. Rev. Lett., 2007, **98**: 262002; arXiv: 0804.4389[hep-ph]